Characterizing spatiotemporal patterns of ground subsidence as an indicator of permafrost thaw in Tso Kar valley, Ladakh using SAR remote sensing

Tara Tripura Mantha, Santonu Goswami

WORKING DRAFT (October 27, 2022)

Characterizing spatiotemporal patterns of ground subsidence as an indicator of permafrost thaw in Tso Kar valley, Ladakh using SAR remote sensing

Tara Tripura Mantha, Santonu Goswami (santonu.goswami@apu.edu.in)

Azim Premji University, Bengaluru, India

ABSTRACT:

Permafrost-related hazards through climate warming-induced degradation are anticipated to increase in the near future. While there is a large community of researchers working on the permafrost landscapes in the Arctic, Tibetan Plateau, and the European Alps, very few studies have looked at the state of permafrost in the Indian Himalayas and hence how these landscapes will change in the near future due to climate warming is quite unknown. Given the dependency of indigenous communities living in these vulnerable landscapes as well as the downstream impacts that this degradation can have on the Ganga and Brahmaputra valleys, it is quite crucial to develop a better understanding of this region in terms of permafrost current and future states. In this pilot study, we make an attempt to characterize permafrost degradation using SAR remote sensing technique to quantify ground subsidence in the Tso Kar area through interferometric analysis. Our results showed that ground subsidence for the snow-free months (June to September) during 2015-2021 ranged from 37 mm to 102 mm. To understand the impact of micro climate on ground subsidence, we explored trends of air temperature, and soil temperature at different depths during 2000-2020 using model-derived data. In both the winter and summer seasons, air and soil temperature (including annual maximum and minimum temperatures) for all depths exhibit a linear increase in temperature suggesting climate warming. This novel approach can provide some new insights into permafrost degradation using ground subsidence as the indicator.

Introduction

Permafrost is an important component of the cryosphere, considered as one among the 54 Essential Climate Variables (ECVs) as recognized by the Global Climate Observing System (GCOS) (GCOS; https://gcos.wmo.int/). ECVs are critical climate parameters which take a major role in characterizing Earth's climate and hence are key variables in providing global-scale climate variability. The permafrost landscape is spread over about 11% of the earth's surface and is one of the largest carbon pools with global soil carbon stock being more than twice the current atmospheric carbon pool. (Schuur 2008, Tarnocai et al 2009, Gruber 2012, Obu et al 2019, Obu

2021). With faster warming rates of temperature in polar and in high-elevated regions, permafrost degradation releases large amounts of greenhouse gasses (GHGs) into the atmosphere causing significant positive feedback to global warming (Pepin et al 2015, Schuur et al 2015, Biskaborn et al 2019). As a consequence, it can lead to catastrophic damage to the ecosystem, infrastructure, and inhabitants (Shur 2007, Streletskiy 2015, Allen 2022). Landscapes underlain by discontinuous or sporadic permafrost are more sensitive to warming temperatures which occupy the majority of Indian Himalayan permafrost (Zhao et al 2010, Obu et al 2019). Although the Global Terrestrial Network for Permafrost (GTN-P) has been monitoring permafrost globally, the scarcity of studies at IH and hence the lack of knowledge about the current state of the permafrost still is worrisome. This is especially true considering the remote mountain communities living in the permafrost regions in the Indian Himalayas and the potential but unexpected permafrost-related hazards in the changing conditions.

Permafrost is thermally defined as ground that remains below 0℃ for 2 or more years. (Harris et al 1988). The energy exchanges between the atmosphere and the ground depict the thermal regime of permafrost landscapes that are used to infer the state of permafrost in the region. Warming temperatures in the permafrost regions cause local ground movements leading to infrastructural damage through slope instability impacting the thermal, mechanical, geomorphic, and hydrologic factors of the landscape, especially in discontinuous ice-rich permafrost regions with reported permafrost-related hazards (Zhao et al 2010, Chadburn et al 2017, Biskaborn 2019). As permafrost degradation is a sub-surface phenomenon, it is often identified through ground subsidence, formation, and expansion of the thermokarst lakes and damage to the infrastructure. (Yang et al 2004, Hinzaman 2005, , Streletskiy, D). Multiple studies carried out over the years have demonstrated that the global permafrost has warmed up over the last three to four decades. (Osterkamp 2003; Hinzman et al., 2005; Wu 2008; Christiansen et al., 2010; Romanovsky et al. 2010; Romanovsky, Vladimir, et al 2010; Smith et al 2010; Slater and Lawrence, 2013; Westermann et al., 2013; Pandey et al 2021). Consequently, slope instability-induced hazards like rock avalanches, destabilized rock glaciers, and unstable mountain slopes are increasingly being reported, perniciously affecting human settlement both directly and indirectly. (Haeberli et al 2017, Hjort et al 2018, MF Azam et al 2019, IPCC 2019, Patton et al 2019, Pandey et al 2021)

With over 76 million people settled in the mountain regions of the Indian Himalayas (IH), it is important to understand the permafrost dynamics of the region (Wester et al 2019). With current estimates, permafrost areas exceed that of glaciers globally and in the IH (Gruber 2017). Climatic conditions in mountain regions are highly heterogeneous and are heavily influenced by local climatic trends. Changes and warming in surface air temperature, precipitation, snow cover, and glacier extent have been observed, indicating the negative impacts of climate change in the region (Dash et al 2007; Bhutiyani et al 2010; Dimri and Dash 2011; Bolch et al 2012; Ren et al 2017, Dimri et al 2021). Table 1: Permafrost study methods adapted from Vonder Mühl et al 2002 and Harris et al 2017. However, systematic in situ permafrost studies in the IH are scarce owing to

their geographical and geopolitical constraints in the region. Regions of the Tibetan Plateau have been extensively studied along with a few regional studies in Pamir, Nepal, Bhutan, and India, Yukon Territory, Gruben rock glacier, and the European Alps. An international program was developed (Global Terrestrial Network for Permafrost, GTN-P) to monitor permafrost using data from 1000 boreholes in Central Asia to expand the understanding of global permafrost dynamics where the nearest borehole site to the Indian Himalayan Region (IHR) is situated at with Aksai Chin (35.4,°79.55 °, elevation: 4827.76 m, permafrost zone: discontinuous) and none within IHR.

Table 01 : A brief list of methods used for permafrost studies and publications that incorporate them.

Drilling	Christiansen et al 2021.
Geophysical and geoelectrical methods	Hauck et al (2004), Moorman et al (2003), Mc Ginnis et al (1973)
GPS surveying	Hu, Yufeng, et al (2022)
Miniature Data loggers	Hoelzle et al (1999)
Bottom temperature of the Snow cover studies	Haeberli (1973)
Refraction seismic	Ikeda (2006)
DC resistivity	King et al (1987)
Ground Penetrating Radar	Munroe et al (2007)
Electromagnetic induction	Maurer and Hauck (2007)
Radiometry	Mühll, Daniel Vonder, et al.

The alpine permafrost regions in IH are remotely situated and are difficult to access.

Satellite remote sensing can be a crucial tool in analyzing the spatial and temporal behavior of permafrost at local to a regional level. Remote sensing-based data and tools have been used to create maps, classify landscapes, classify vegetation, identify the climate change impacts on

polar regions, monitor landforms, and detect land deformations such as ground subsidence (Kääb 2008, Dong et al 2013, Jorgenson et al 2016).

In this study, we use the Synthetic Aperture Radar (SAR) interferometric technique to quantify ground subsidence at Tso Kar valley, Ladakh India. This study is an exploratory attempt to map the ground subsidence of our study area using a series of SAR interferograms acquired over a period of 7 years (2015-2021). As SAR images are highly dependent on the dielectric properties of the sensing area, we acquire images during snow-free months (June - October).

Our main objectives to achieve in this study are to:

- Characterize ground subsidence for summer months in the study area using SAR interferometry.
- Characterize long term trends of climate parameters in the study area
- Investigate relationships between climatic parameters (such as air surface temperature, soil temperature at different depths,) and land subsidence

Our Science Questions:

- What are the spatiotemporal characteristics of ground subsidence in our study area?
- Are there any relationships of long-term climate patterns to ground subsidence in the study area?
- Which among the considered local climate parameter affects subsidence the most?

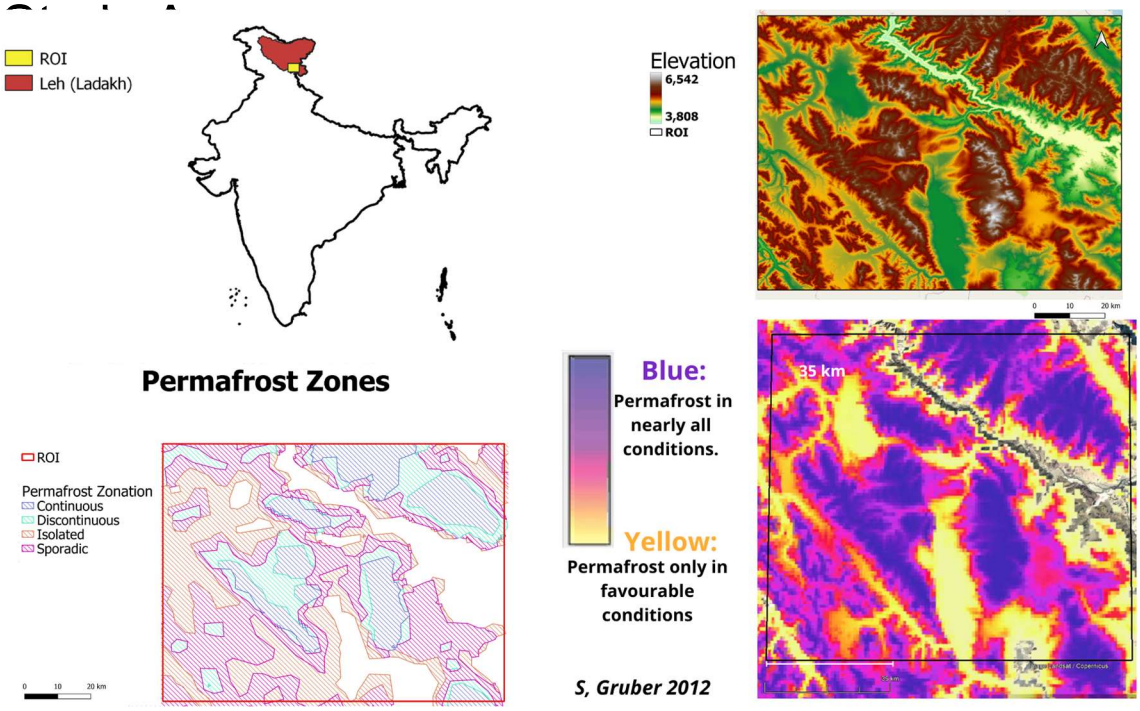

Fig 01: Overview of study region. (a) Geographical location (b) DEM obtained from SRTM3 (c) Permafrost zonation based on Obu et al 2019 (d) Permafrost zonation index based on S Gruber 2012. Sources:

Geography:

Ladakh is a newly administered union territory surrounded by the Zanskar range located in the Trans-Himalayan region. The area of interest (AOI) in this study is a rectangular region spanning an area of 9151 km^2 with elevations ranging from 3764 to 6517 m a.s.l including the Tso Kar and Tso Startspuk basin formed through the Tso Kar - Telecon Fault. (ON Bhargava 1989). The area is surrounded by a few local mountain communities that depend on the landscape for cattle grazing, hydrology, and transportation. It is situated near Tanglangla Pass, one of the highest mountain passes in the world serving as a bridge that avails goods and facilities to the most remote places. The lithology of the area comprises sedimentary rocks and basalts, dominated by thin marble banded phyllites and schist with a desert- steppe vegetation. (Chowdhary and Rao 1990, Negi 1995, Klimes 2003). Despite being a cold and arid region, the area has numerous species of life recorded :139 species of birds, 232 species of vascular plants, up to 10 species of mammals, and 2 species of reptiles.

The presence of permafrost is confirmed through the presence of ice lenses in the Borehole drilling

that has reported the occurrence of permafrost zones of depth ranging from 0.1 to 13.2 m, at depths up to 29 m (Rastogi 1999). Permafrost models categorize the permafrost condition in the study region to be present in all conditions to favorable conditions with an estimated Active Layer Thickness of 0.1 to 4.2m. (Gruber 2008, Obu 2019, Wani 2020). At a regional scale, permafrost is influenced by micro-climatic factors such as elevation, bedrock properties, snow cover, vegetation, and amount of organic material. In-situ measurements to obtain climate information are scarce. Climatic information is summarized in Table 02 and paleoclimate is summarized in Table 03.

(https://rsis.ramsar.org/RISapp/files/RISrep/IN2443RIS_2012_en.pdf)

Climatology

The climate at Ladakh resembles dry arctic with low rainfall during both summer and winter monsoon with negative moisture (Kramer et al. 2004). Thus, the definition of seasons is slightly varied (Pre-Monsoon: April-May-June AMJ; Monsoon: June-July-August JJA; Post monsoon : October-November ON; Winter : December-January-February-March DJFM) with the one as defined by the Indian Meteorological Department (Pre-monsoon: MAM; Southwest Monsoon: JJAS; Post-Monsoon: OND; Winter: JF) (Cevuturi et al 2018, annual report- https://mausam.imd.gov.in/imd_latest/contents/ar2021.pdf) while October- April is defined as winter in one study (Bhattacharyya 1988). From a 60 year long measurement of climatic parameters at a weather station situated at 3500 m asl, the regional climate graph shows the climate to be relatively arid from end of march to October and relatively humid during the rest of the year with May, June and September having absolute minimum temperature below 0 degree celcius (Miehe et al 2001).

Table - 02: Summary of climate data as obtained from published results for Ladakh region. MAAT refers to mean annual air temperature.

Study	Period	Minimum Temperature (C)	Maximum temperature (C)	Rainfall (annual)	MAAT	Mean Annual Temperature
A Bhattacharya et al (1989)	1931- 1960	-40 to -20	-	-	-	-
Philip and Mazari (2000)	2000	-	30	-	-	-
Meterological station at 34.09'N, 77 34'E (Miehe et al	60 years	-13.4 -28.8 (absolute	-	83mm	-	5.7

2001)		)				
Meterological station at 34.09'N, 77 34'E (Demske et al 2009)	1931 to 1960	-14.0	24.7	115mm	-	5.5
Meterological station at 34.09'N, 77 34'E (Thayyen and Dimri 2014)	2010-2012	-23.4	33.9	-	-	-

Table - 03: Paleoclimate at and around Tso kar data from late glacial period, mostly focusing on Tso Kar basin including surrounding basins. The table is constructed from Demske, 2009

Timeline (Kyr BP)	**Region**	**Notable climatic condition**
15.2 – 13 (Late glacial)	Tso Kar (TK)	· High alpine cold desert, dry and cold climate · Low precipitation (ppt) · Low melt-water supply during winter
15 (Late glacial)	South Ladakh	· Stronger summer monsoon
13.8 – 13.0 (Late glacial)	TK	· Dry climate pulses
12.8 -12.5 (Late glacial)	Ladakh	· Strengthened monsoonal circulation

12.5 – 11.8 (Late glacial)	TK	· Weakened summer monsoon · Reduced summer ppt
11.8 – 4.8 (Early to mid-Holocene)	TK	· Increased monsoonal rainfall · Increased monsoonal length
10.5 – 9.5 (Early to mid-Holocene)	Pangong Co	· Major humid pulse
8.4 – 8.0 (Early to mid-Holocene)	Ladakh	· Abrupt decrease in temperature
8.0 – 6.9 (Early to mid-Holocene)	TK	· Dry climatic conditions
7.2 / 7 (Early to mid-Holocene)	Pangong Co	· Start of aridity
6.9 – 4.8 (Early to mid-Holocene)	TK basin	· 2nd humid pulse
4.8 – 3.7 (Late Holocene)	TK	· Abrupt transition to aridity · Dry vegetation cover · Weakening of summer monsoon
3.1 – 1.3	TK	· Dry and cool climatic condition
1.3 to later	TK	· Improved moisture condition

Methods

Date Used

Climate Data from Giovanni

We use FLDAS_NOAH001_G_CA_D modeled data to obtain climatic geophysical parameters : Surface air temperature (Tair), Soil temperature for depths 0-10 cm, 10-40 cm, 40-100 cm, 100-200cm(T0-10, T10-40, T40-100, T100-200) from Giovanni as developed by the Goddard Earth Sciences Data and Information Services Center (GES DISC). To align with ROI, the bounding box used for the extraction of past climate data is (77.7436,32.7127,78.8449,33.5437). The data is a time series averaged over the area from 2001-2020 for all the parameters. We have also obtained data for all the parameters specifically on the dates corresponding to Sentinel-1 acquisition data used in this study for the purpose of exact analysis. In order to identify snow-free months (Fig.2(c)), we have also obtained snow depth data for the same bounding boundary from 2015-2020. We chose the duration of June-September to be snow-free duration to align with IMD definition.

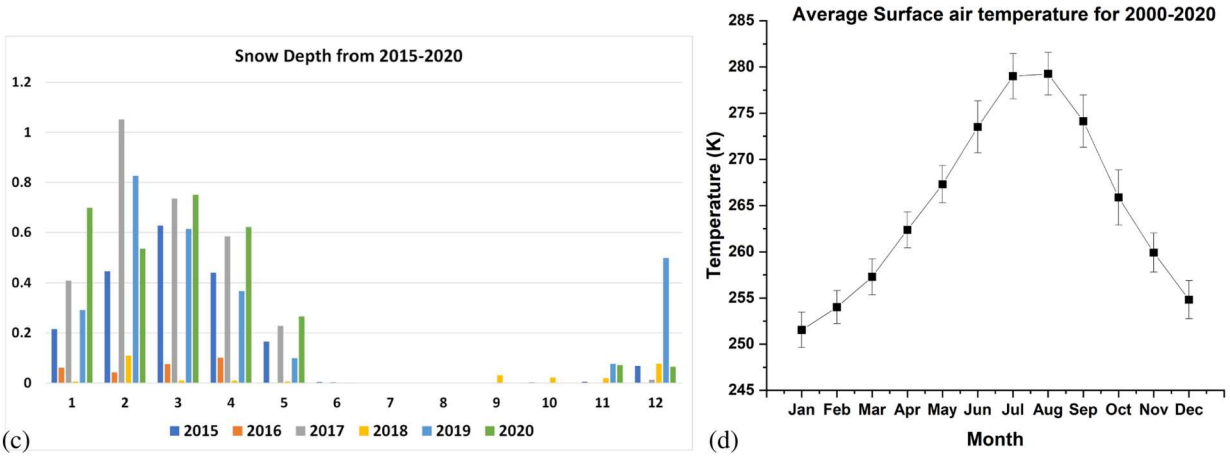

Fig 2: (c) Area averaged Snow depth (m) from NOAH modelled data from January 2015 to December 2020 for study for ROI. (d)Area-averaged monthly air temperature averaged from 2000-2020

Sentinel-1 Data Used

In this study, a total of 14 Single Look Complex (SLC) images are obtained with sensor mode being Interferometric Wide Swath (IW) during snow-free months for this region (June-September, Fig 1c). These images are processed to obtain 6 interferograms using European Space Agency's (ESA) SeNtinel Application Platform (SNAP) for a total of 4 bursts, bounding Tso moriri at the southmost burst. However, 3 of the interferograms are not chosen for further analysis due to poor coherence.The sentinel-1 image processing is divided into four processes. An interferogram is generated between two SAR satellite imagery at two different times, the earlier being the master image and the latter being the slave image.

Table 04: Stack of Sentinel 1 images obtained

Year Month	2017	2019	2020
Image (Master)	01-June	03-June	21-June
Image (Slave)	05-September	07-September	13- September

Satellite Data processing using SNAP

Provide a description of the SNAP TOOL

All the following figures should be integrated into one as a workflow because that is what it is

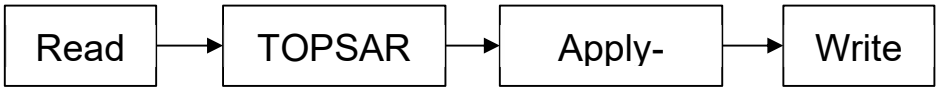

Process 1: Pre-processing of sentinel 1 images

We pre-process the images by selecting appropriate number of bursts (here,4) through TOPSAR split to include AOI. We further proceed to preserve image information such as satellite velocity and position. Apply-orbit-file

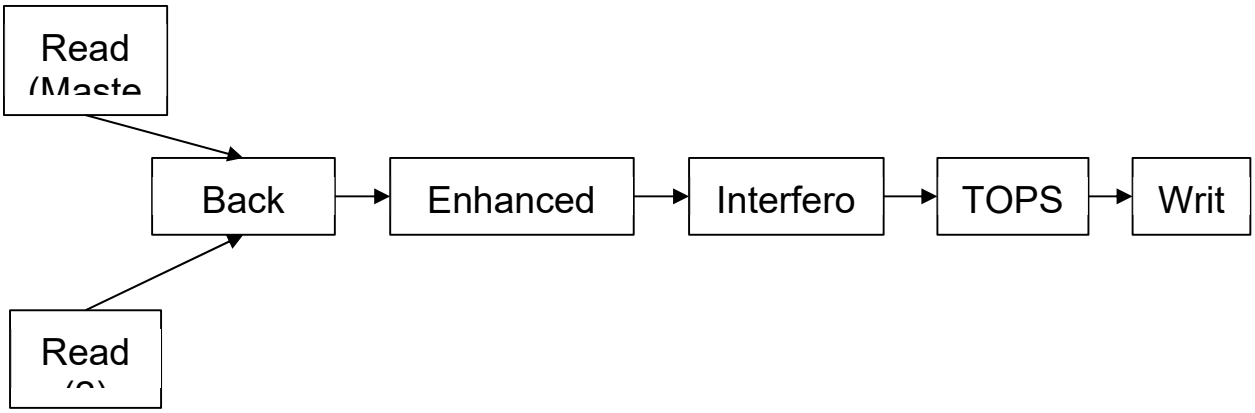

Process 2: Coregistration and computation of interferrogram

In Process 2, coregistration is one of the crucial step to permform interferrogram analysis (Wang et al 2011). Through back-geocoding, the same pixel in both the images is made sure to correspond to the same ground target, Enhanced spectral diversity increases the accuracy in phase, thus leading to the generation of a more coherent interferogram. To remove the black lines that result from TOPSAR imaging, we apply Topsar- Deburst attain a spatially continuous image.

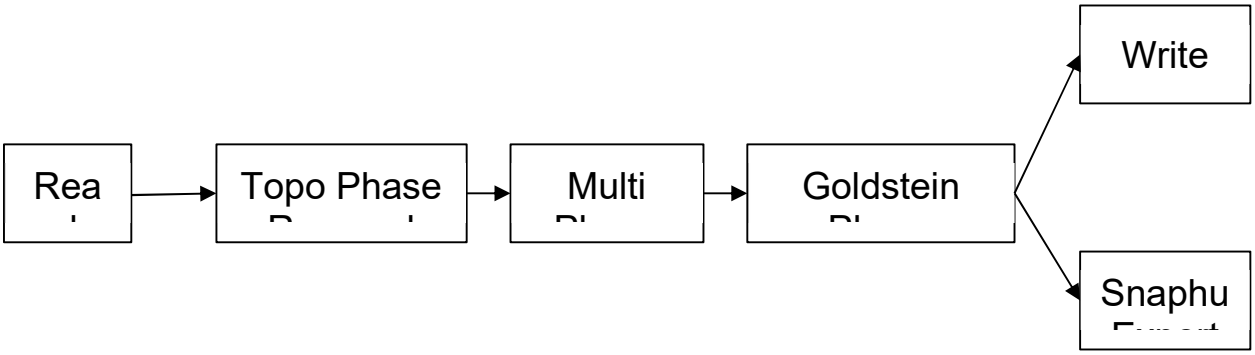

In process 3, the interferogram obtained is refined through the removal of phase contribution due to topography, phase contribution through ground scatterers (speckle-noise reduction), and further reducing noise in phase through the Goldstein phase filtering technique. This product is then exported to carry out unwrapping through snaphu export

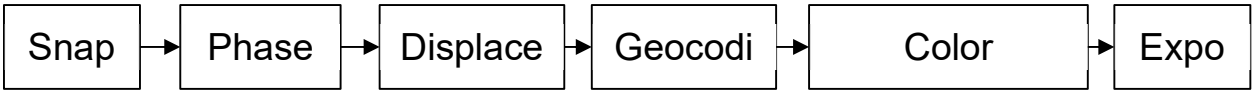

In the final process, process 4, the flattened phase image is unwrapped which recovers the integer number of cycles that should be added to wrapped phase. As a result, the unambiguous phase value for each pixel is obtained. This unambiguous phase information is then converted in terms of height displacement. Geocoding assigns geological coordinates to the respective pixel through. Geometric distortion arising due to side looking radar is removed through terrain

correction. The obtained image is then subjected to the removal of low coherent values and choosing an apt color panel for better confidence in results obtained.

Statistical analysis

Results

Subsidence

Sentinel-1 interferograms generated between June and September of the corresponding year were used to compute displacement for the entire study area. While most of the place undergoes uplift, we have observed subsidence of upto ~6 cm i.e 10.21 cm, 6.98 cm and 6.75 cm respectively for 2017,2019 and 2020. Most of the area have values missing due to poor coherence (< 0.4). Area around Tso Kar lake where presence of permafrost has been confirmed also shows subsidence but the magnitude is small ~2 cm. The isolated and sporadic zonation of permafrost could limit the occurrence of subsidence with higher magnitudes. There is significant increase in subsidence area as well as magnitude of subsidence during 2019 when compared to 2017. For 2020, overall, the area shows minimal subsidence. Histogram of displacement (subsidence and uplift) for the three years shows that while most of the region undergoes subsidence, but for 2020, more than 50% of the region is uplifted.

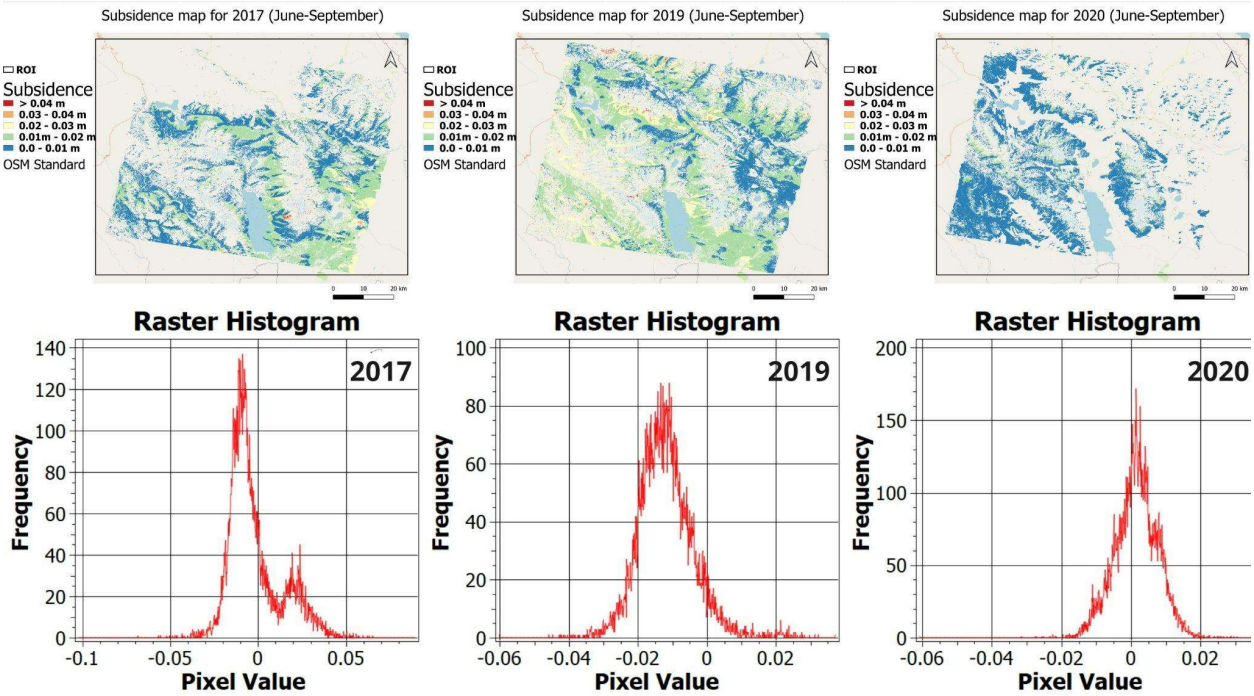

——————————————————choosing the better picture——————————————————

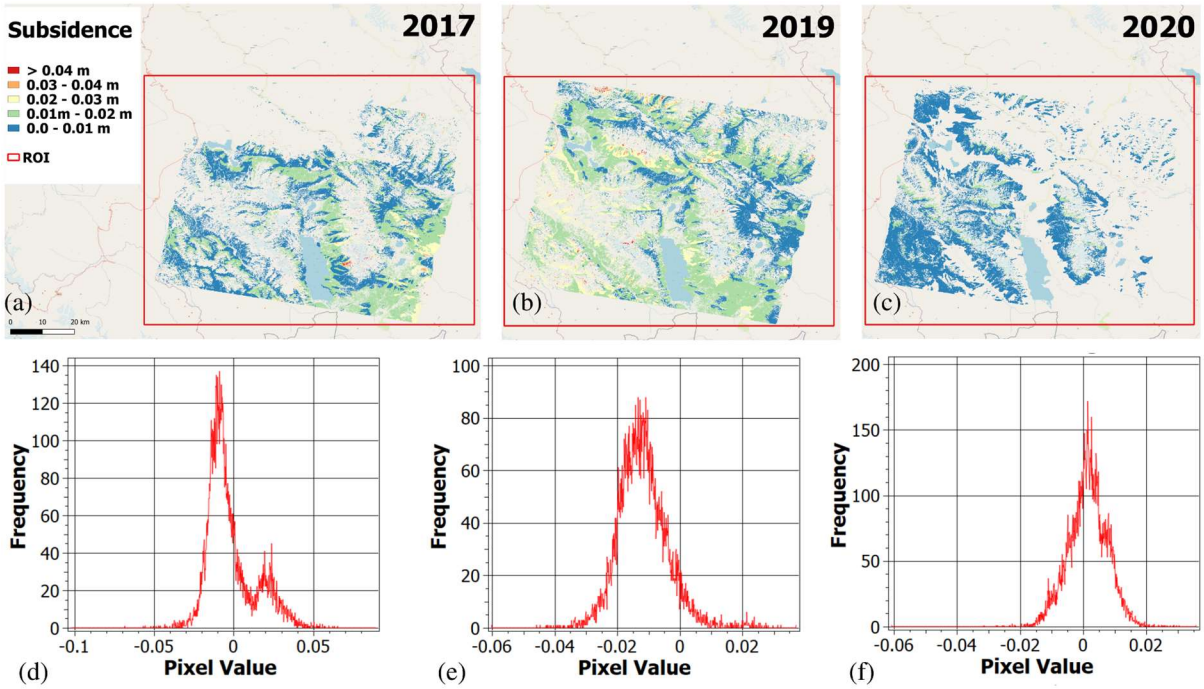

Fig 3: (a) Subsidence map over study area including Tso Kar and Tso Startspuk from Sentinel-1 InSAR from 2017 to 2020. (b) Histogram showing frequency distribution of subsidence and uplift for the entire study area.

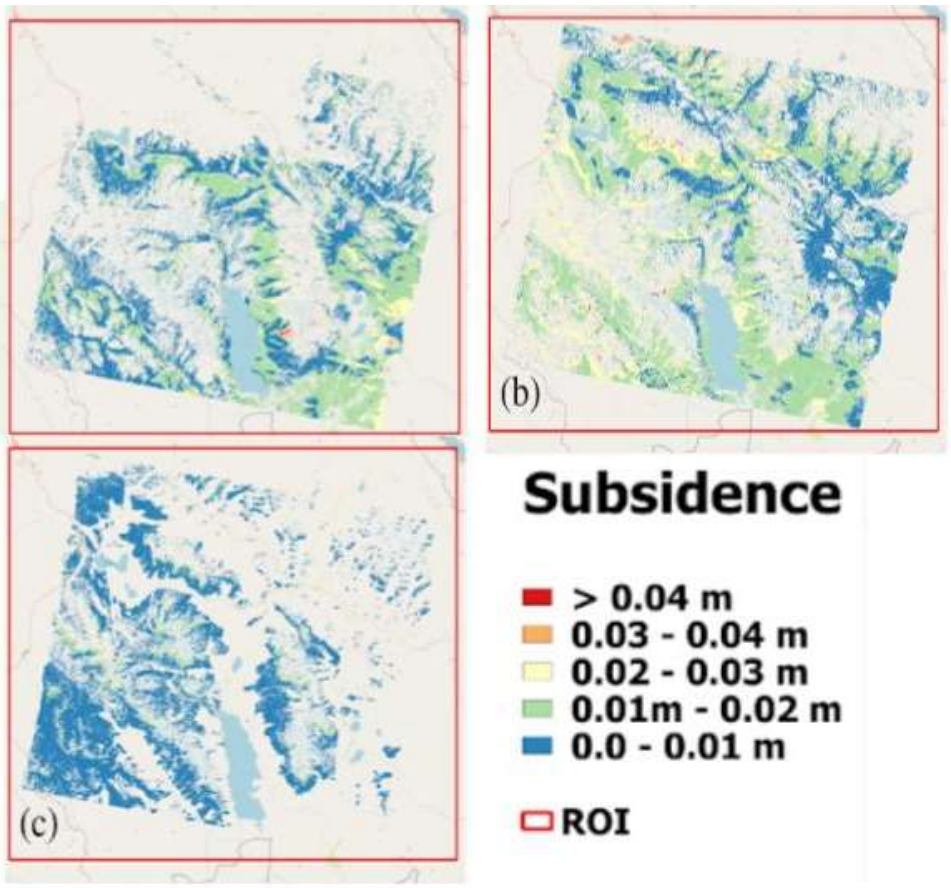

Air and soil temperature

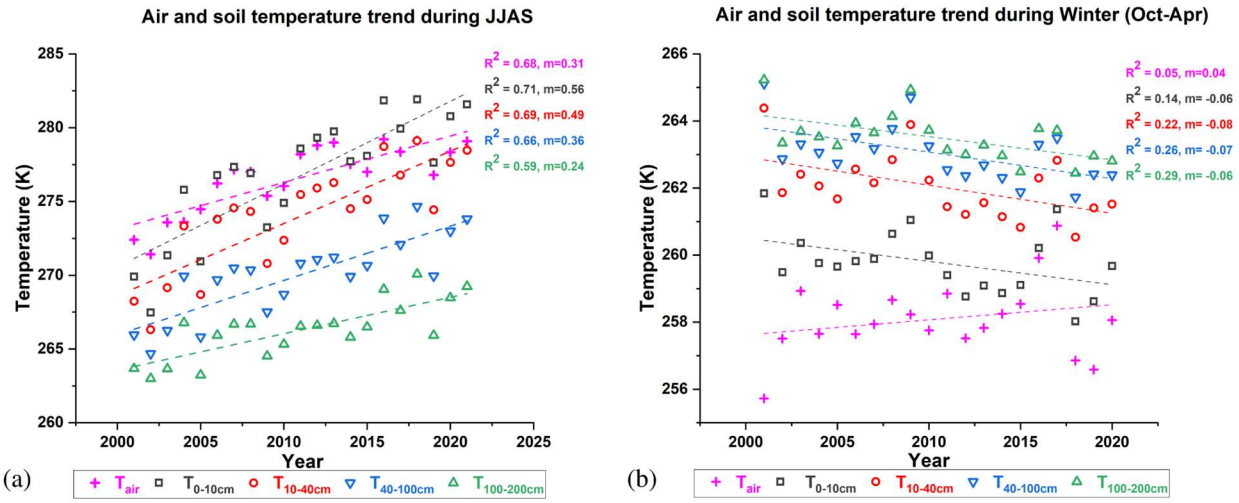

Fig 3: Area averaged Air and Soil temperature at different depths pattern for (a) JJAS and (b) Winter. The dashed lines represent best linear fit relation of the modelled data.

We obtain long term trend for air temperature and soil temperature at different depths, averaged over entire study area using FLDAS_NOAH001_G_CA_D model from 2000 to 2021 particularly for two major time periods: JJAS (a) and locally defined winter (Oct-Apr: (b)). We observe a warming trend for all the parameters for JJAS with decrease in the rates of increasing temperatures over the years with increase in depth. However, we see similar decreasing rate for soil temperature at different depths. In case of air temperature, we observe winter warming up in the past 20 years.

Air temperature and soil temperature at different depths are observed for the same acquisition dates as of SAR images as mentioned in table 03. We obtain spatial distribution of slope to analyze the rate of change at each pixel and the same is repeated for subsidence. Air temperature shows an increase in temperature (positive slope values) over the entire study area, while no such homogenous spatial behavior is observed for soil temperature. With increasing depths, the rate of warming is spreading spatially but this behavior discontinues for soil temperature at depth of 100-200 cm.

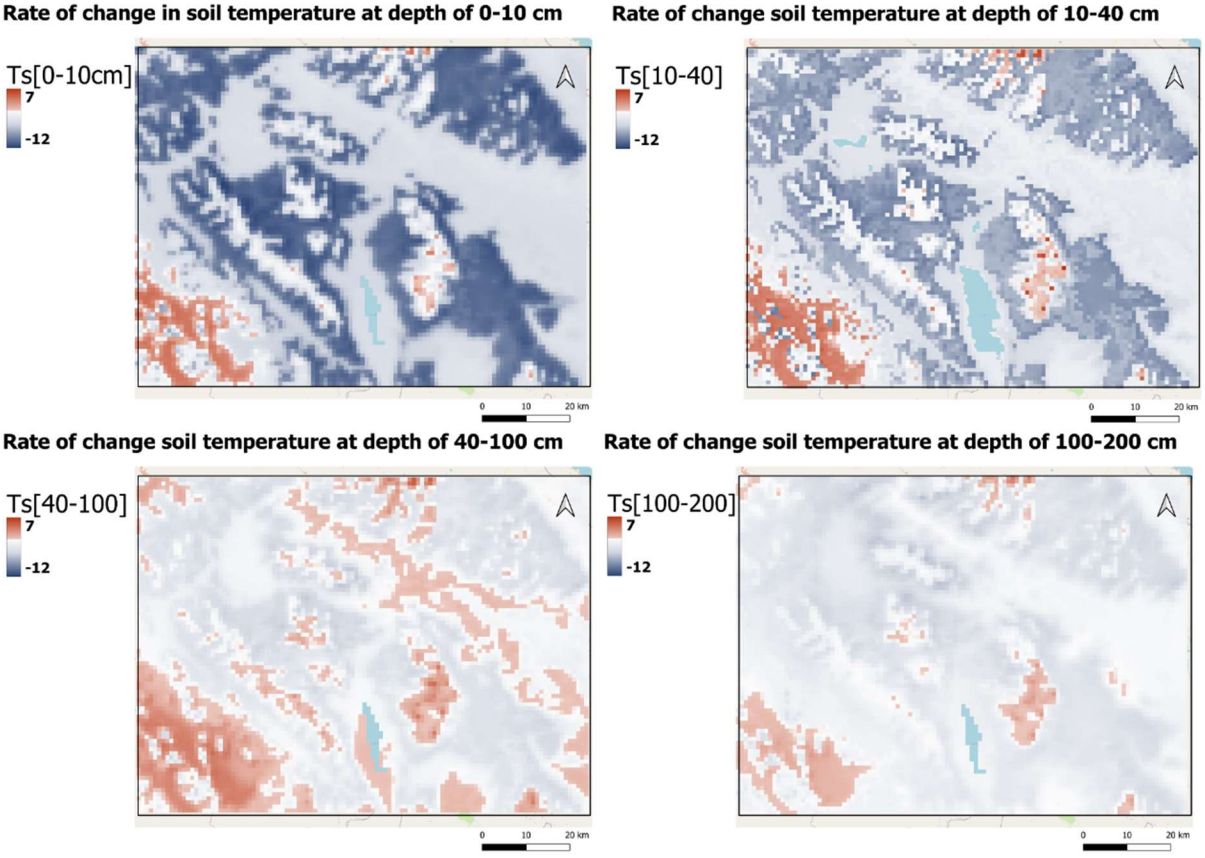

Fig 4: Pixel-wise rate of change in soil temperature at different depths for 2017,2019 and 2020
What is the rate here ?every two years or every year? -
If you write “rate of change…” in the figure legend, you can get rid of this phrase from the figure and just write soil temperature at depth….

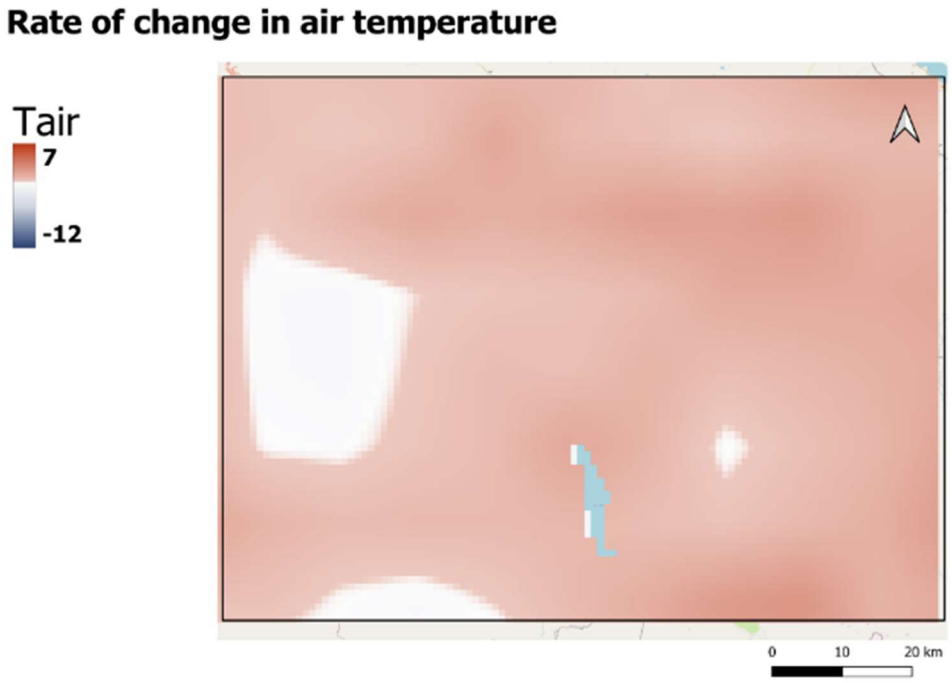

Discussions

Subsidence as permafrost degradation

Long term behaviour has shown warming of air temperatures over the past 20 years. In mountain regions, permafrost is strongly dependent on regional parameters such as vegetation, soil moisture, soil temperature, elevation, soil organic matter. We explore this dependency through corelation analysis among the rates of change in the regional parameters in fig 06. As we obtained subsidence for three years that show subsidence over a large region of study area (coherence >= 0.4), we observe the rate of change in temperatures for the same time period as subsidence. The correlation observed is weak which can be attributed to low data points. Furthermore, fig 05 shows temporal behaviour of subsidence that shows areas with positive slope i.e areas where subsidence has increased from 2017 to 2020, the corresponding standard deviation is high. Thus, no specific temporal behaviour can be associated to subsidence in the region.

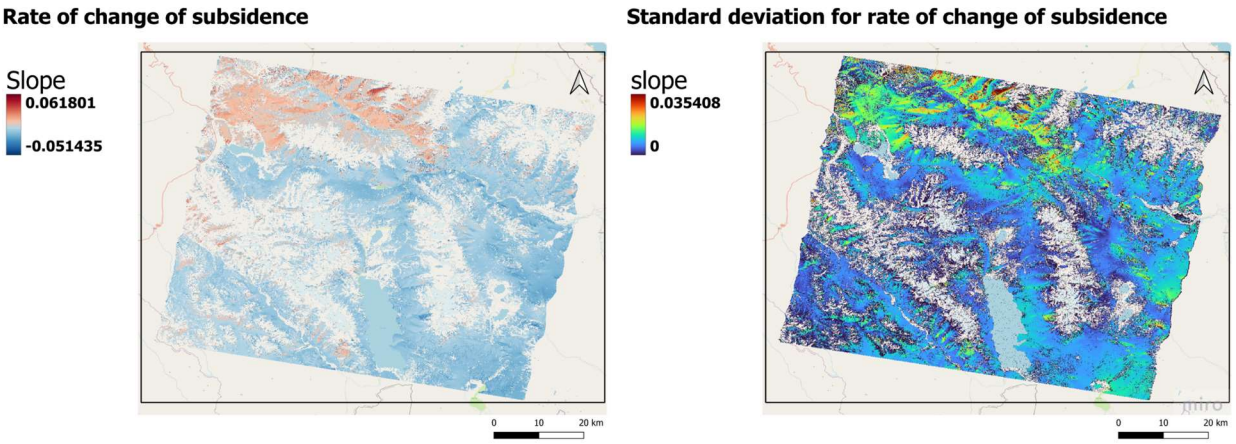

Fig 05: rate of change of subsidence and standard deviation of subsidence.

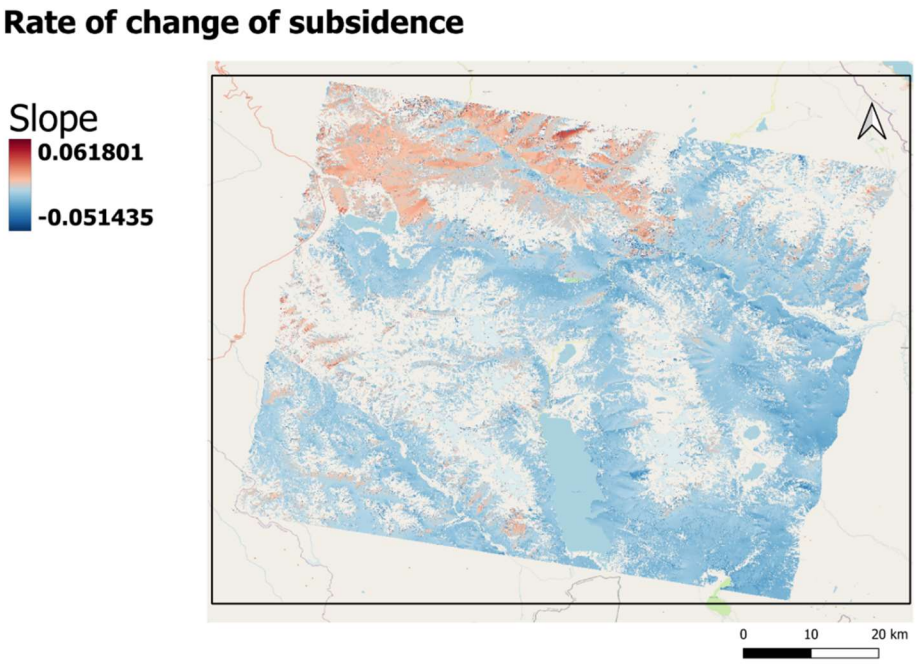

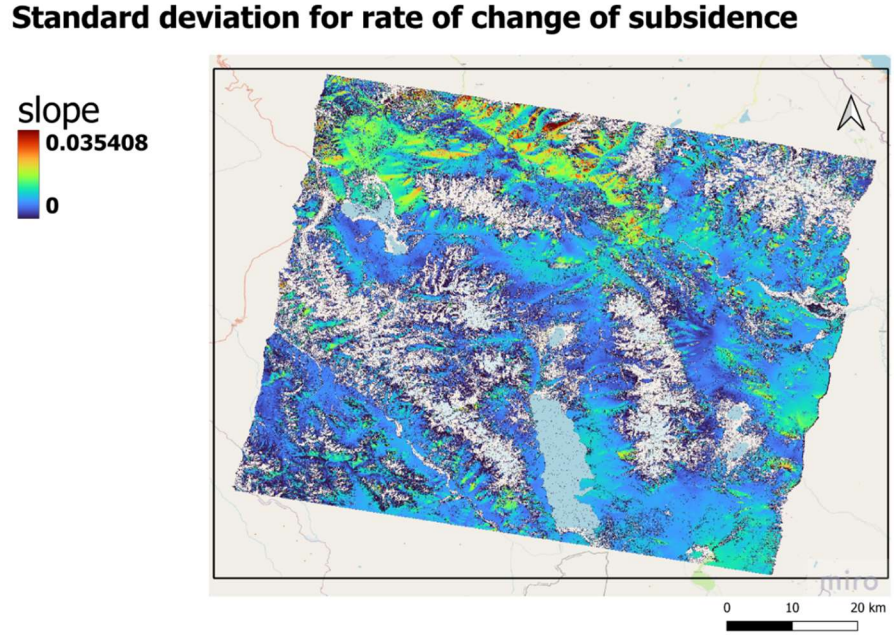

Spatially, out of the considered parameters, we see a higher correlation between subsidence-elevation and between subsidence- soil temperature at depth 0 to 10 cm. This relation is of importance as it reveals thermal regime of ground in permafrost regions which is essential to estimate permafrost degradation through increase in active layer thickness (Wani et al 2019). The study area also has periglacial landforms such as cryogenic hummocks were spotted during a short field visit.

Fig 06: Correlation between elevation and the rate of change in local climate parameters in consideration (subsidence, Tair: Air temperature, Ts[0-10]: soil temperature at 0-10 cm,Ts[10-

40]: soil temperature at 10-40 cm,Ts[40-100]: soil temperature at 40-100 cm,Ts[100-200]: soil temperature at 100-200 cm).

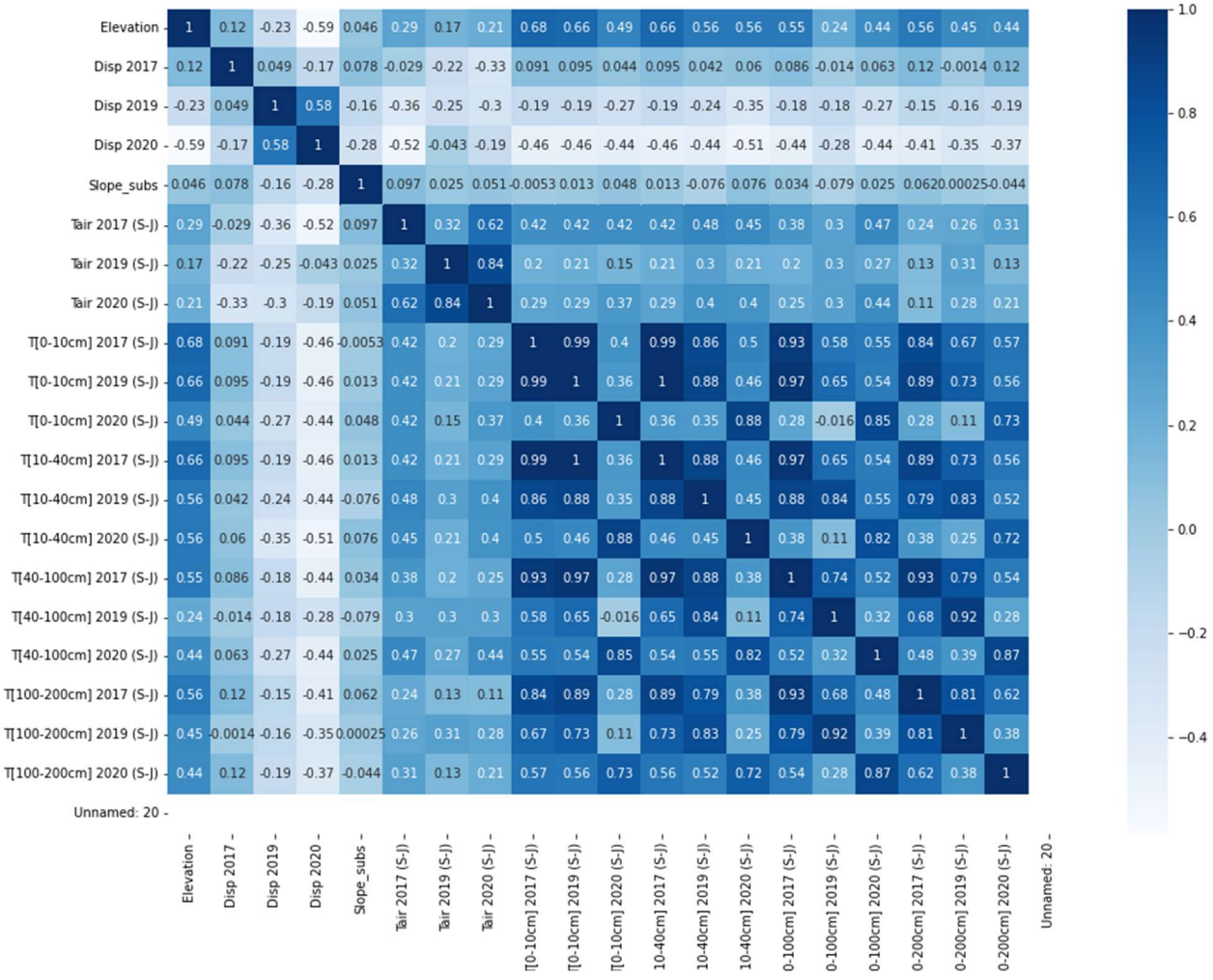

Conclusions

Understanding the state of permafrost in mountain regions is crucial to the entire population that is dependent on the Indian himalayas. A knowledge gap in inferring climate change impact on permafrost can avoid building resilience to permafrost related hazards. This study is a first of its kind to observe ground subsidence in the permafrost area of the Indian Himalayas.

Our study suggests that spatial and temporal characteristic of subsidence can be succesfully obtained using sentinel-1 interferrometry. As the study region is situated in the mountain areas of the Himalayan region, subsidence of a few centimeters as observed in this study can cause a significant slope instability. One of the world's highest pass, Tanglang la is situated at close proximity and extension of subsidence analysis in human infrastructure present areas can help in building sustainability, resilience and adaptation to the observed climate warming. Use of sentinel data along with the modelled data can be further used in developing the understanding of the permafrost dynamics at regional scale.

References:

1. https://www.mdpi.com/2072-4292/12/18/3029/htm
2.
3. "GCOS | WMO." GCOS | WMO, gcos.wmo.int/en/essential-climate-variables/table. Accessed 8 Sept. 2022.
4. **Alphabetical order**
5. Allen, Simon, et al. "Assessment principles for glacier and permafrost hazards in mountain regions." Oxford Research Encyclopedia of Natural Hazard Science. 2022.
6. Bhargava, O. N. "Holocene tectonics south of the Indus Suture, Lahaul-Ladakh Himalaya, India: a consequence of Indian Plate motion." Tectonophysics 174.3-4 (1990): 315-320.
7. Bhattacharyya, A. "Vegetation and climate during the last 30,000 years in Ladakh." Palaeogeography, Palaeoclimatology, Palaeoecology 73.1-2 (1989): 25-38.
8. Bhutiyani, M. R, Vishawas S. Kale, and N. J. Pawar. "Climate change and the precipitation variations in the northwestern Himalaya: 1866–2006." International Journal of Climatology: A Journal of the Royal Meteorological Society 30.4 (2010): 535-548.
9. Biskaborn, Boris K., et al. "Permafrost is warming at a global scale." Nature communications 10.1 (2019): 1-11.
10. Bolch, Tobias, et al. "The state and fate of Himalayan glaciers." Science 336.6079 (2012): 310-314.
11. Chadburn, S. E., et al. "An observation-based constraint on permafrost loss as a function of global warming." Nature Climate Change 7.5 (2017): 340-344.

12. Chevuturi, A., A. P. Dimri, and R. J. Thayyen. "Climate change over Leh (Ladakh), India." Theoretical and Applied Climatology 131.1 (2018): 531-545.
13. Christiansen, Hanne H., et al. "Ground ice content, drilling methods and equipment and permafrost dynamics in Svalbard 2016–2019 (PermaSval)." SESS report 2020-The State of Environmental Science in Svalbard-an annual report 3 (2021).
14. Demske, Dieter, et al. "Late glacial and Holocene vegetation, Indian monsoon and westerly circulation in the Trans-Himalaya recorded in the lacustrine pollen sequence from Tso Kar, Ladakh, NW India." Palaeogeography, Palaeoclimatology, Palaeoecology 279.3-4 (2009): 172-185.
15. Dèzes, Pierre. (1999). Tectonic and Metamorphic Evolution of the Central Himalayan Domain in Southeast Zanskar (Kashmir, India). Mémoires de Géologie (Lausanne). 32.
16. Dimri, A. P., et al. "Climate change, cryosphere and impacts in the Indian Himalayan Region." Current Science (2021).
17. Dong, P., Wang, C., Ding, J., 2013. Estimating glacier volume loss using remotely sensed images, digital elevation data, and GIS modelling. International Journal of Remote Sensing 34, 8881e8892
18. Gruber, S. Derivation and analysis of a high-resolution estimate of global permafrost zonation. Cryosphere 6, 221–233 (2012)
19. Gruber, Stephan, et al. "Inferring permafrost and permafrost thaw in the mountains of the Hindu Kush Himalaya region." The Cryosphere 11.1 (2017): 81-99.
20. Haeberli, Wilfried, Yvonne Schaub, and Christian Huggel. "Increasing risks related to landslides from degrading permafrost into new lakes in de-glaciating mountain ranges." Geomorphology 293 (2017): 405-417.
21. Harden, J. W. et al. Field information links permafrost carbon to physical vulnerabilities of thawing. Geophys. Res. Lett. 39, L15704 (2012)
22. Harris, Charles, et al. "Permafrost and climate in Europe: Monitoring and modelling thermal, geomorphological and geotechnical responses." Earth-Science Reviews 92.3-4 (2009): 117-171.
23. Harris, S.A. (1988). The alpine periglacial zone, In: Clark, M.J. (ed). Advances in periglacial geomorphology, 363–372. John Wiley & Sons.
24. Hinzman, L.D., Bettez, N.D., Bolton, W.R. et al. Evidence and Implications of Recent Climate Change in Northern Alaska and Other Arctic Regions. Climatic Change 72, 251–298 (2005).
25. Hjort, Jan, et al. "Degrading permafrost puts Arctic infrastructure at risk by mid-century." Nature communications 9.1 (2018): 1-9.
26. Hoelzle, Martin, Matthias Wegmann, and Bernhard Krummenacher. "Miniature temperature dataloggers for mapping and monitoring of permafrost in high mountain areas: first experience from the Swiss Alps." Permafrost and periglacial processes 10.2 (1999): 113-124.

27. Hu, Yufeng, et al. "Ground surface elevation changes over permafrost areas revealed by multiple GNSS interferometric reflectometry." Journal of Geodesy 96.8 (2022): 1-19
28. IPCC in Climate Change 2013: The Physical Science Basis. Contribution of Working Group I to the Fifth Assessment Report of the Intergovernmental Panel on Climate Change (eds Stocker, T. F. et al.) 1535 (Cambridge Univ. Press, 2013).
29. Jorgenson, Mark Torre, and Guido Grosse. "Remote sensing of landscape change in permafrost regions." Permafrost and periglacial processes 27.4 (2016): 324-338.
30. Kääb, Andreas. "Remote sensing of permafrost-related problems and hazards." Permafrost and periglacial processes 19.2 (2008): 107-136.
31. Miehe, Georg, et al. "The Climatic Diagram Map of High Asia: Purpose and Concepts (Klimadiagramm-Karte von Hochasien. Konzept und Anwendung)." Erdkunde (2001): 94-97.
32. Mühll, Daniel Vonder, et al. "New geophysical methods of investigating the nature and distribution of mountain permafrost with special reference to radiometry techniques." Permafrost and Periglacial Processes 12.1 (2001): 27-38.
33. Obu, J. "How much of the earth's surface is underlain by permafrost?." Journal of Geophysical Research: Earth Surface 126.5 (2021): e2021JF006123.
34. Obu, Jaroslav, et al. "Northern Hemisphere permafrost map based on TTOP modelling for 2000–2016 at 1 km2 scale." Earth-Science Reviews 193 (2019): 299-316.
35. Pepin, et al. "Elevation-dependent warming in mountain regions of the world." Nature climate change 5, no. 5 (2015): 424-430.
36. Osterkamp, T. E. "Establishing long-term permafrost observatories for active-layer and permafrost investigations in Alaska: 1977–2002." Permafrost and Periglacial Processes 14.4 (2003): 331-342.
37. Pandey, Pratima, et al. "Cause and process mechanism of rockslide triggered flood event in Rishiganga and Dhauliganga River Valleys, Chamoli, Uttarakhand, India using satellite remote sensing and in situ observations." Journal of the Indian Society of Remote Sensing 49.5 (2021): 1011-1024.
38. Patton, Annette I., Sara L. Rathburn, and Denny M. Capps. "Landslide response to climate change in permafrost regions." Geomorphology 340 (2019): 116-128.
39. Philip, G., and R. K. Mazari. "Shrinking lake basins in the proximity of the Indus Suture Zone of northwestern Himalaya: a case study of Tso Kar and Startsapuk Tso, using 1RS-1C data." International Journal of Remote Sensing 21.16 (2000): 2973-2984.
40. Rastogi, S. P., and S. Narayan. "Permafrost in the Tso Kar Basin, Ladakh." Proceedings of the Symposium for Snow, Ice and Glaciers. 1999.
41. Ren, Yu-Yu, et al. "Observed changes in surface air temperature and precipitation in the Hindu Kush Himalayan region over the last 100-plus years." Advances in Climate Change Research 8.3 (2017): 148-156.
42. Romanovsky, Vladimir E., et al. "Thermal state of permafrost in Russia." Permafrost and Periglacial Processes 21.2 (2010): 136-155.

43. Romanovsky, Vladimir E., Sharon L. Smith, and Hanne H. Christiansen. "Permafrost thermal state in the polar Northern Hemisphere during the international polar year 2007–2009: a synthesis." Permafrost and Periglacial processes 21.2 (2010): 106-116.
44. Schuur, Edward AG, et al. "Climate change and the permafrost carbon feedback." Nature 520.7546 (2015): 171-179.
45. Schuur, Edward AG, et al. "Vulnerability of permafrost carbon to climate change: Implications for the global carbon cycle." BioScience 58.8 (2008): 701-714.
46. Shur, Yu L., and M. Torre Jorgenson. "Patterns of permafrost formation and degradation in relation to climate and ecosystems." Permafrost and Periglacial Processes 18.1 (2007): 7-19.
47. Slater, Andrew G., and David M. Lawrence. "Diagnosing present and future permafrost from climate models." Journal of Climate 26.15 (2013): 5608-5623.
48. Smith, S. L., et al. "Thermal state of permafrost in North America: a contribution to the international polar year." Permafrost and Periglacial Processes 21.2 (2010): 117-135.
49. Streletskiy, D., O. Anisimov, and A. Vasiliev. "Chapter 10—Permafrost Degradation." Snow and Ice-Related Hazards, Risks and Disasters; Shroder, JF, Haeberli, W., Whiteman, C., Eds: 303-344.
50. Streletskiy, Dmitry, Oleg Anisimov, and Alexander Vasiliev. "Permafrost degradation." Snow and ice-related hazards, risks, and disasters. Academic Press, 2015. 303-344.
51. Tarnocai, Charles, et al. "Soil organic carbon pools in the northern circumpolar permafrost region." Global biogeochemical cycles 23.2 (2009).
52. Thayyen, R. J., and A. P. Dimri. "Factors controlling Slope Environmental Lapse Rate (SELR) of temperature in the monsoon and cold-arid glacio-hydrological regimes of the Himalaya." The Cryosphere Discussions 8.6 (2014): 5645-5686.
53. Van Everdingen, R., 2005. Multi-language glossary of permafrost and related ground-ice terms, National Snow and Ice Data Center/World Data Center for Glaciology, Boulder, World Wide Web Address: http://nsidc. org/fgdc/glossary.
54. Vonder Mühll, Daniel, Christian Hauck, and Hansueli Gubler. "Mapping of mountain permafrost using geophysical methods." Progress in Physical Geography 26.4 (2002): 643-660.
55. Wani, John Mohd, et al. "Single-year thermal regime and inferred permafrost occurrence in the upper Ganglass catchment of the cold-arid Himalaya, Ladakh, India." Science of the Total Environment 703 (2020): 134631.
56. Wester, Philippus, et al. The Hindu Kush Himalaya assessment: mountains, climate change, sustainability and people. Springer Nature, 2019.
57. Westermann, Sebastian, et al. "Transient thermal modeling of permafrost conditions in Southern Norway." The Cryosphere 7.2 (2013): 719-739.
58. Wu, Qingbai, and Tingjun Zhang. "Recent permafrost warming on the Qinghai-Tibetan Plateau." Journal of Geophysical Research: Atmospheres 113.D13 (2008).

59. Yang, Meixue, et al. "Desertification and its relationship with permafrost degradation in Qinghai-Xizang (Tibet) plateau." Cold Regions Science and Technology 39.1 (2004): 47-53.
60. Zhang, Tingjun, et al. "Statistics and characteristics of permafrost and ground-ice distribution in the Northern Hemisphere." Polar Geography 23.2 (1999): 132-154.
61. Zhao, Lin, et al. "Thermal state of permafrost and active layer in Central Asia during the International Polar Year." Permafrost and Periglacial Processes 21.2 (2010): 198-207.
62. Schuur, Edward AG, et al. "Vulnerability of permafrost carbon to climate change: Implications for the global carbon cycle." BioScience 58.8 (2008): 701-714.
63. Field CB, Raupach MR, eds. 2004. The Global Carbon Cycle: Integrating Humans, Climate, and the Natural World. Washington (DC): Island Press.
64. Khan, Abul Amir, et al. "The Himalayan cryosphere: A critical assessment and evaluation of glacial melt fraction in the Bhagirathi basin." Geoscience Frontiers 8.1 (2017): 107-115.
65. Dong, P., Wang, C., Ding, J., 2013. Estimating glacier volume loss using remotely sensed images, digital elevation data, and GIS modelling. International Journal of Remote Sensing 34, 8881e8892
66. Bauder, Andreas, et al. "Winter Accumulation Measurements on Alpine Glaciers using Ground Penetrating Radar." 2018 17th International Conference on Ground Penetrating Radar (GPR). IEEE, 2018